MODELING THE CATHODIC REGION IN CREVICE CORROSION UNDER A THIN ELECTROLYTE FILM INCLUDING PARTICULATES

Arun S. Agarwal[1], Uziel Landau[1], Xi Shan[2] and Joe H. Payer[2]

[1] Department of Chemical Engineering

[2] Department of Material Science and Engineering

Case Western Reserve University

10900 Euclid Ave, Cleveland OH, 44106 USA

Crevice corrosion may be limited by the capacity of the external cathodic region to support anodic dissolution currents within the crevice. The analysis here focuses on behavior of metal surfaces covered by a thin (~microns) layer of the electrolyte film including particulates. The particulates can affect the cathode current capacity (I_{total}) by increasing the solution resistance ("volume effect") and by decreasing the electrode area ("surface effect"). In addition, there can be particulate effects on oxygen reduction kinetics and oxygen transport. This work simulates and characterizes the effect of a uniform particulate monolayer on the cathode current capacity for steady state conditions in the presence of a thin electrolyte film. Particulate configurations with varying particle size, shape, arrangement, volume fraction, and electrode area coverage were numerically modeled as a function of the properties of the system. It is observed that the effects of particles can be fully accounted for in terms of two corrections: the volume blockage effect on the electrolyte resistivity can be correlated using Bruggeman's equation, and the electrode coverage effect can be modeled in terms of a simple area correction to the kinetics expression. For the range of parameters analyzed, applying these two correction factors, cathodes covered with thin electrolyte films that contain particles can be represented in terms of equivalent homogenous electrolytes that can then be analyzed using simpler approaches. Continuing work will examine the effects of greater volume fractions of particles and multiple particle layers.

Keywords: Crevice corrosion, cathode, particulates, effective conductivity, area coverage, modeling, thin film

INTRODUCTION

Crevice corrosion may occur in restricted regions due to transport limitations, followed by a build-up of a highly corrosive chemistry, capable of dissolving the metal. The present state of understanding of localized corrosion of passive metals is based primarily upon analysis of fully immersed electrodes. There has been limited analysis of the localized corrosion in moist layers of dust, particulates, and deposits. Previous related analytical (1, 2) and numerical (3) studies have focused on galvanic corrosion where the rates of the anodic and cathodic processes are comparable, analyzing mostly the effects of the electrode kinetics and the thickness of the electrolyte layer. Depending upon the size, shape and kinetics of anodic dissolution of the metal, the anode imposes a total current demand. The external exposed cathode surface needs to provide this current for

sustaining the localized corrosion process. The capacity of the cathode to sustain corrosion depends on the electrolyte properties and oxygen reduction kinetics on the cathode surface. In the case of thin electrolyte films that contain particulates, the ability of the cathode to sustain localized corrosion can be significantly altered.

OBJECTIVE

The presence of particulates on the cathode surface can significantly reduce the cathode capacity (I_{total}) by increasing the ohmic resistance to current flow in solution and by decreasing the electrode area. In addition, particulates can affect the oxygen reduction kinetics and its transport. In this work, the particulate effects on the current distribution are analyzed on the macroscopic scale by applying 'effective' properties to homogeneous electrolyte systems, and on the microscopic scale, using detailed distributions around single particles and particle arrays. Results by the two methods are compared.

The objectives of this work are (i) to model and simulate the cathode current capacity in presence of a uniform particulate monolayer (on the cathode) at steady state and (ii) to compare the cathode capacity for the heterogeneous particulate (in electrolyte) configurations to simulation results for homogeneous electrolyte systems incorporating approximations for effective conductivity (using Bruggeman's equation) and electrode area blockage by the particles. The total current which a specific cathode with known particulate distribution can provide to sustain the crevice corrosion, is calculated numerically for limiting potential conditions set at the crevice opening.

APPROACH

The analysis is based upon data for stainless steel (SS 316L) due to the extensive literature available on its electrochemical polarization and localized corrosion properties. The schematic of the cyclic potentiodynamic polarization (CPP) curve for stainless steel is given in Fig. 1. The potential where the reverse scan intersects the forward scan is defined as the repassivation potential, E_{rp}. At potentials more negative than the repassivation potential, crevice corrosion will not occur (4). The repassivation potential (E_{rp}) for stainless steel is more negative than the measured corrosion potential (E_{corr}) in natural seawater (5), indicating that the alloy could undergo crevice corrosion spontaneously. Hence, the crevice mouth is held at the repassivation potential (E_{rp}), and cathodic current distributions in the potential window between the E_{rp} and E_{corr}, designated as the active corrosion region in the schematic (Fig. 1), are simulated. For a freely corroding system, the most positive potential is E_{corr}, and the most negative potential at the crevice opening is E_{rp} to sustain crevice corrosion of SS 316L.

The decoupled cathodic region from a crevice corrosion system is shown in Fig. 2. The anodic crevice gap is represented by a virtual anode on the left, and the opening of the crevice is fixed at the repassivation potential (E_{rp}). This virtual anode is assigned a primary current distribution (no anode kinetics or mass transfer effects present) thus providing a constant current to the cathodic region on the metal surface outside of the crevice. Such an approach makes it possible to study the effect of various process parameters separately on the cathode, and independent of anodic reactions. The assumption made here is that the anode dissolution products formed inside the crevice do not affect the solution properties and/or reduction kinetics on the external cathode

surface. In our earlier work (6), current and potential distributions were modeled based on this decoupled model in a homogeneous electrolyte (no particulates) as a function of the geometry, solution properties, pH and reduction kinetics. A similar study employing the decoupled cathode model was also done by Cui et. al (7). In their recent work (8), they used a decoupled anode to determine the anode current demand as a function of the crevice geometry. By equating this anodic current to cathode capacity for homogeneous electrolytes, Cui et. al indicated probable conditions for crevice corrosion.

The decoupled cathode treatment is used here to model the effect of particles on cathode current capacity. Fig. 3 (a) shows a schematic of particulates distributed on the cathode of a crevice system. A non-uniform distribution of irregularly shaped particles is depicted. This system is represented in terms of an idealized system for modeling purposes incorporating the following constraints:

- Uniform particle distribution
- Steady state
- A single monolayer of particles with $\text{height}_{particle} = \text{thickness}_{electrolyte}$
- No chemical changes considered

A uniform distribution of particles of predetermined size, shape and arrangement is incorporated in a thin electrolyte film covering the cathode surface, and the current and potential distributions are modeled around these particles (Fig. 3 (b)). The particles are inert, of the same height as the electrolyte film. Although such a system does not exactly match the real system, it provides an initial point for modeling current and potential distributions. The following particulate parameters are varied and their effect on the cathode capacity (I_{total}) is determined:

- Particle size
- Particle arrangement on the cathode (Fig. 9)
- Particle shape
- Electrode area coverage ($A_{active}/A_{geometric}$)
- Volume fraction blockage ($V_{solution}/V_{total}$)

METHODOLOGY

The steps involved in simulating a particulate system are shown schematically in Fig. 4. First, a particle of known size and shape is selected. Then the distribution of the particles on the cathode surface is assigned by placing a number of particles equidistant to each other and to the edges of the finite cathode. The width of the cathode is kept sufficient to accommodate a single particle array and its associated gaps next to the edges. Due to symmetry, only one half of the gap between the particle rows is assigned on each side of the sectioned row that is being modeled. It would have been sufficient to model only one half of the particle row (with one half of its associated gap), however, in order to increase the clarity of the graphical results, the entire particle array (rather than its half) has been modeled. The surfaces of the particles are set as insulators, since they are inert.

Once the geometry is fixed, the effects of the macroscopic scale parameters, including the length of the cathodic region (L_c) and the film conductivity (1.2 – 121 mS/cm) on the

current and potential distributions are simulated. A range of electrode kinetics ($i_o = 10^{-7}$ to 10^{-11} A/cm^2) and repassivation potentials (E_{rp} = -0.56 to -0.11 V_{NHE}) is explored including data typical to oxygen reduction kinetics on stainless-steel (5).

In an attempt to derive a less complex representation of the system that is amenable to simpler treatment, we seek to represent the particulate system (that must be analyzed by comprehensive 3-D modeling) by a simpler equivalent system. It is hypothesized that the particulates affect the system mostly through two effects: (i) a volumetric effect due to increased ohmic resistance to current flow by solution blockage, and (ii) a surface-interfacial effect due to coverage of a portion of the electrode area by particles. To account for these effects, we introduce separate corrections for each of the two effects:

- The bulk electrolyte blockage decreases the equivalent conductivity of the system. Bruggeman's equation (9) is applied to account for this phenomenon:

$$k_{eff} = k(1 - \phi_{particles})^{\frac{3}{2}}$$ [1]

where;

$$\phi_{particles} = \frac{V_{particles}}{V_{solution} + V_{particles}}$$ [2]

- The change in the oxygen reduction kinetics on the cathode due to partial coverage of the electrode area by the particulates is accounted for by correcting the value of the exchange current density, i_o, in the cathode kinetics expression (Eq. [6] below). This correction is based on recognizing that the kinetics expression incorporates a current density term which is defined in terms of the entire electrode area ($A_{geometric}$), yet in reality, the particles block a portion thereof [Area (particle base)].

$$\frac{A_{active}}{A_{geometric}} = \frac{\text{Area(geometric) - Area(particle base)}}{\text{Area(geometric)}}$$ [3]

where

Area(particle base) = No. of particles x (electrode area covered by each particle) [4]

Instead of introducing a correction to the current density, i, it is preferable, due to computational considerations, to define an equivalent exchange current density':

$$i_o' = i_o \text{ x } A_{active}/A_{geometric}$$ [5]

The cathode capacity obtained from the simulations carried out in the simpler, equivalent, homogeneous electrolyte systems employing the above corrections are compared with the cathode capacities obtained by 3-D modeling of the heterogeneous particulate/electrolyte configurations based on the actual shape, size and distribution of the inert embedded particles.

Cathodic Polarization Behavior: The oxygen reduction current density (i_c) distribution on the cathode is modeled using Tafel kinetics. The Tafel equation in the absence of mass transfer limitation is;

$$i_c = -i_0 * \exp\{-(\alpha_c F/RT)[V^{cathode} - E_0^{cathode} - \Phi]\} \qquad [6]$$

where Φ is the ohmic potential drop in solution.

The thermodynamic potential for oxygen reduction kinetics is given by;

$$E_0^{cathode} = +0.19 \text{ V} \quad \text{(for SS 316L (5))} \qquad [7]$$

No external potential is applied on the cathode since it is assumed to be a freely corroding system, i.e.

$$V^{cathode} = 0 \text{ V} \qquad [8]$$

In presence of oxygen mass transfer limitation, the cathode current density is given by;

$$i_c = -\cfrac{1}{\cfrac{1}{i} + \cfrac{1}{i_L}} \qquad [9]$$

where;

$$i = i_0 * \exp\{(\alpha_c F/RT)(E_0^{cathode} + \Phi)\} \qquad [10]$$

and

$$i_L = \frac{nFD_{eff}C_b}{\delta} \qquad [11]$$

Under oxygen mass transport limitations, the maximum current density (= limiting current, i_L) that the cathode can provide is fixed according Eq. [11]. C_b is the bulk concentration of oxygen (based on its solubility which is a function on salinity and temperature), δ is the thickness of the mass transfer boundary layer which can be approximated to be the thickness of the stagnant electrolyte layer (G_f), and D_{eff} is the effective diffusivity of oxygen. For the case of diffusion through a liquid film which contains particulates, the effective diffusivity of oxygen depends on the porosity (1 - $\phi_{particles}$) and tortuosity (τ) of the particulate layer through which oxygen must diffuse (10).

$$D_{eff} = D_{O_2}\frac{(1-\phi_{particles})}{\tau} \qquad [12]$$

The shape of the particles determines the value of the tortuosity (τ). Hence, spherical particles ($\tau = 3$ (11)) exert a larger mass transfer limitation as compared to cubic particles ($\tau = 1$) even if the particles occupy the same volume fraction in solution. Eq. [12] was derived for a multi-layer particle configuration. In the absence of a more suitable model, we apply this expression, recognizing that the empirically determined value of τ could be adjusted to fit the particulate monolayer system which is considered here. The greater the volume fraction of the particles ($\phi_{particles}$), the lower the effective diffusivity, thus increasing the mass transfer limitation.

Virtual Anode: Primary current distribution with no kinetics or transport limitations is assumed to prevail on the virtual anode. The potential of the virtual anode at the crevice opening is fixed, and is equal to the repassivation potential (E_{rp}).

$$\Phi_{anode} = E_{rp} \qquad [13]$$

The virtual anode within the crevice serves as a source of current to the cathodic region outside of the crevice.

Bulk Solution: A stagnant thin film electrolyte with a uniform solution conductivity (κ) is considered. The oxygen concentration at the top (air interface) of the thin electrolyte layer is assumed to be constant ($C_b = 0.25$ mM). The bulk diffusivity of oxygen ($D_{O2} = 1.8 \times 10^{-5}$ cm^2/s) is also assumed to be constant. For the situations where oxygen transport limitations are considered, diffusional transport through the thin electrolyte film is assumed. Under these conditions Laplace's equation for the potential is solved in the solution (Eq. [14]) to provide the steady state potential and current distribution on the cathode surface.

$$\nabla^2 \Phi = 0 \qquad [14]$$

Simulation Software: The 3-D simulations of current and potential distribution for the cathode with electrolyte that contains particles were done using FEMLAB® (12). The geometry was first constructed and then the boundary conditions for the two electrodes (Eq. [6] or [9] for the cathode and Eq. [13] for the anode) were applied and Laplace's equation ([14]) solved in the bulk solution. FEMLAB® uses a finite element algorithm that self adjusts the grid size to produce higher density elements next to corners and edges, where the current and potential fields change the most.

The 2-D simulations in homogeneous electrolyte were done using a dedicated electrochemical modeling CAD software, CELL-DESIGN® (13). This software solves the potential field subject to the complete Butler-Volmer equation as a boundary condition at the cathode. The kinetic parameters viz. the exchange current density (i_0), the charge transfer coefficients (α_a and α_c) and the reversible potential (E_0) are entered in the program. The software also takes into account the mass transfer limitation by calculating the limiting current based on the bulk concentration of oxygen (C_b), the mass transfer boundary layer thickness (δ), which was set equal to the electrolyte film thickness, G_f, and the effective diffusivity of oxygen (D_{eff}).

RESULTS AND DISCUSSION

A typical particle distribution on the cathode is shown in Fig. 5. The particles selected are 25 μm cubes. The height of the electrolyte layer (G_f) is kept equal to the height of the particles. The particles are placed equidistant to each other and to the edges of the cathode segment. The depicted uniform arrangement of particles creates an electrode area fraction ($A_{active}/A_{geometric}$) of 0.306 and a volume fraction ($V_{solution}/V_{geometric}$) of 0.306. Current and potential distributions modeled in this particulate system (based on the process parameters in Table I) are depicted in Fig. 6.

TABLE I: Kinetics and geometrical parameters used in the simulation of electrolyte films with 25 μm cubic particles ($A_{active}/A_{geometric}$ = 0.306, $V_{solution}/V_{geometric}$ = 0.306).

E_o V_{NHE}	i_o A/cm^2	α_c	E_{rp} V_{NHE}	E_{cor} V_{NHE}	i_L A/cm^2	κ mS/cm	G_a μm	G_f μm	L_C cm
0.19	10^{-9}	0.59	-0.31	0.09	2.2×10^{-4}	1.21	25	25	0.18

The arrows in the current plot of Fig. 6 indicate the direction and magnitude of current flow in the solution. It is observed that the maximum current is generated by the exposed cathode area close to the virtual anode (crevice opening), and only a small fraction of the total reduction current is produced by the major portion of the cathode away from the crevice opening. For the case considered in Fig. 6, 75% of the current is provided by 50% of the electrode area adjacent to the anode. The potential distribution in solution (Fig. 6) indicates a considerable loss in solution potential in the region close to the crevice opening, which confirms the large current seen in the same region in Fig. 6. The potential drop is minimal for the remainder of the cathode. Here, 83% of the potential drop in solution occurs in the first 50% of the cathode region adjacent to the anode.

Effect of the Cathode Length on the Cathode Current Capacity: The cathode capacity of the particulate system described above is simulated as a function of the length of the cathode (L_C) using the process parameters given in Table I with the exception that κ = 12.1 mS/cm. The cathode capacity values are plotted in Fig. 7 in terms of $I_{3-D,particle}$ as a function of L_C. The cathode capacities obtained for homogeneous electrolyte systems without particulates, by 2-D simulations using (i) only the Bruggeman's correction for adjusting the bulk conductivity ($I_{2-D, Bruggeman}$), (ii) only the area correction to account for the electrode area lost by particle coverage ($I_{2-D, area}$) and (iii) both, the Bruggeman's and area corrections ($I_{2-D, area + Bruggeman}$) are also plotted as a function of cathode length in Fig. 7. It is seen that simulations of the homogeneous electrolyte systems incorporating the volume (Bruggeman) and surface coverage (area) corrections reproduce accurately the cathode capacity obtained by 3-D simulation of the particulate system. However, either the area or volume corrections by themselves are insufficient in predicting the cathode capacities in the range explored. As the length of the cathode increases beyond 0.1 cm, the potential drop due to solution resistance becomes appreciable, and the area correction alone cannot predict the cathode capacity. On the other hand, just employing the correction for the bulk conductivity using Bruggeman's equation significantly overestimates the cathode capacity. Similar results were obtained for runs made without considering any mass transfer limitations (using Eq. [7]). The cathode capacity

approaches a saturation value for longer cathodes. This result in the presence of particulates is consistent with the trends observed in homogeneous electrolyte without particulates (5).

Effect of the Process Parameters on the Cathode Capacity in the Presence of Particulates:
The cathode capacity of the particulate system discussed above is simulated for varying bulk solution conductivity (κ = 1.21 x10^{-1} to 1.21 x 10^{-3} S/cm), oxygen reduction kinetics (i_O = 10^{-7} to 10^{-11} A/cm^2) and repassivation potential (E_{rp} = -0.56 to -0.11 V$_{NHE}$). The above parameter ranges are chosen since they incorporate the general chemical and electrochemical properties of systems encountered in atmospheric corrosion of stainless steels. The results are compared with cathode capacities obtained by simulations of the homogeneous electrolyte incorporating volume and area corrections as shown in Fig. 8. The simulation parameters are the same as listed in Table I. In this case too, we find that the simulations of the homogeneous electrolyte, with volume and area corrections adequately predict the cathode capacities obtained by 3-D modeling of the particulate system. The process parameters were varied to explore a range of conditions:

- when slow kinetics (low i_o) and high solution conductivity (low solution potential drop) were applied, the interfacial kinetics or available electrode surface area becomes important in determining the cathode capacity of the system
- for high solution resistance (low κ) and fast kinetics (high i_o), the volume fraction of solution available for current flow strongly affects the cathode capacity,
- for a large driving force (E_{rp} much more negative than $E_{o,c}$) the cathodic current density is greatly increased, and the cathode region close to the crevice opening has a large effect on the total cathode capacity.

Across the entire range of parameters studied, the presence of a uniform distribution of particles on the cathode does not change the trends in the average current density distributions, which remain similar to those seen for homogeneous electrolyte solutions. The corrections for the loss of electrode area and the change in effective conductivity due to presence of particles are sufficient to predict the trends and the magnitudes of the cathode capacities.

Effect of Mass Transfer Limitations on the Cathode Capacities for Particulate configurations: The I_{total} values for the particulate system discussed above were obtained using the process parameters given in Table I (with the exception that κ was set to 12.1 mS/cm) with and without mass transfer limitations (Fig. 9). It is seen that the mass transfer effects are significant for large potential driving force (highly negative E_{rp}), fast kinetics (large i_o) and high solution conductivity (large κ). For all these conditions, there is a significant increase in the cathode current capacity. Although a large driving force for high current density exists near the crevice mouth, the limiting current density is all that can be realized. Under such conditions, mass transfer limitations are encountered close to the crevice opening, where the current density tends to be high. Due to mass transfer limitations, the maximum current density is limited (= i_L) and the current capacity of the cathode region is lower than that encountered when mass transfer limitations are not present. For conditions where the limiting current is not reached (slow kinetics, large resistance to current flow due to low conductivity and more positive E_{rp}), the cathode capacities with and without mass transfer limitations are essentially equal.

Effect of Particle Arrangement on the Cathode Capacity: Fig. 10 shows the current capacity of the cathode plotted as a function of the length of the cathode (using the simulation parameters listed in Table I with the exception that κ was set to 12.1 mS/cm) for two different particle arrangements. The increase in effective path length for current flow in the case of the non-linear arrangement does not significantly change the cathode capacity from the one observed for the linear arrangement. The simulation of the homogeneous electrolyte system with the corrections for volume and area effects adequately predicts the cathode capacity. Thus, changing the arrangement of the particles on the cathode surface has an insignificant effect on the total cathode capacity.

Effect of the Volume Fraction and the Area Coverage on the Cathode Capacity: Simulations were run for three different particulate configurations with different area and volume fractional coverage (Table II).

TABLE II: Geometrical parameters used in the 3-D simulation of the cathode with varying particulate area and volume coverage.					
Case No.	Height of particles, h_p [μm]	Length of base of particles, L_{baseP} [μm]	Height of electrolyte film, G_f [μm]	Fractional electrode area available for reaction ($A_{active}/A_{geometric}$)	Fractional solution volume available for current flow ($V_{solution}/V_{geometric}$)
1	10	25	25	0.889	0.889
2	20	25	25	0.556	0.556
3	25	25	25	0.306	0.306

The shape and arrangement of the particles were kept the same. The particles had a square base, and their height was equal to the height of the electrolyte layer. Applying the base parameters in Table I, with the exception that κ was set to 12.1 mS/cm, cathode capacities were calculated as a function of the length of the cathode. Simulations on an equivalent homogeneous electrolyte system with area and volume corrections were also done. The cathode capacities are plotted for each of the 3 cases. Fig. 11 indicates that the cathode capacity is a strong function of both the area as well as volume coverage by the particles. The cathode capacity is the lowest for the largest area and volume coverage and vice versa. The simulations of the equivalent homogeneous electrolyte system with volume and area corrections correctly predicted the cathode capacity of all the cases considered. In Fig. 12 (a), the ratio of the cathode capacity in the presence of particulates ($I_{3-D,particle}$) to the one obtained in homogeneous electrolyte (without area and volume corrections, I_{2-D}) is plotted as a function of the length of the cathode. This ratio remains almost constant over the entire length of the cathode, as long as the volume and area fractional coverage are fixed. For high volume fraction and high area fraction coverages, the cathode capacity in the presence of particulates is a small fraction of the total current obtained for homogeneous electrolyte ($\sim$ 23 % for $A_{active}/A_{geometric} = V_{solution}/V_{geometric} = 0.306$). Fig. 12 (b) indicates that the fractional cathode capacity, which is plotted for a constant cathode length of 0.36 cm, increases almost linearly with decrease in area and volume fraction of the particulates. This trend might not be representative of cases where the area and volume fractions occupied by the particles are not equal to each other.

CONCLUSIONS

Cathode current capacities were simulated for a variety of particulate configurations subject to the conditions of (i) uniform particle distribution, (ii) monolayer coverage, (iii) $A_{active}/A_{geometric} \geq 0.3$, (iv) $V_{solution}/V_{total} \geq 0.3$, and (v) steady state with no chemical changes in the electrolyte. Particles in the electrolyte exhibit both volumetric (solution) and cathode area (interfacial kinetic) effects. The shape and arrangement of particles has negligible effect on the total cathode current. Mass transport limitations become significant under conditions for high cathode capacities. Most of the contribution to the current is close to the anode, which is similar to the trends observed for a homogeneous electrolyte layer. The cathode capacities with particulates were compared to those obtained by modeling of the equivalent homogeneous electrolyte corrected for the volume effect (using an effective conductivity based on the Bruggeman's equation) and the surface area effect (by adjusting the kinetics on the cathode). The simulation results of the equivalent homogeneous electrolyte system adequately predict the cathode capacity in the presence of particulates over a wide range of physical, chemical and electrochemical properties that are generally encountered in atmospheric corrosion. For the range of properties and conditions analyzed here in thin electrolyte layers that contain particles, the cathode capacities can be represented by 2-D simulations of homogeneous electrolyte systems with properly adjusted properties. This 2-D modeling is relatively undemanding as compared to 3-D modeling of particulate configurations based on the shape and size of the particles.

ACKNOWLEDGEMENT

REFERENCES

1. R. Morris, W. Smyrl, *J. Electrochem. Soc.* **136** 3229 (1989).
2. E. McCafferty, *J. Electrochem. Soc.* **124** 1869 (1977).
3. P. Doig, P.E.J. Flewitt, *J. Electrochem. Soc.* **126** 2057 (1979).
4. L. M. Calle, R.D. Vinje, and L.G. MacDowell, *J. Corr. Sci & Eng.* **6** C013 (2003).
5. N. Sridhar, C.S. Brossia, D.S. Dunn, A. Anderko, *Corrosion* **60** 915 (2004).
6. A. Agarwal, U. Landau, and J. Payer, to be submitted (2005).
7. F. Cui, F. J. Preseul-Moreno, R. G. Kelly, *Corrosion Science* accepted May, 2005. (invited).
8. F. Cui, F. J. Preseul-Moreno, R. G. Kelly, *ECS Trans.*, **1**, Oct. (2005).
9. D. A. G. Bruggeman, *Ann. Phys. Leipzig* **24** 636 (1935).
10. F. Brilhac , F. Bensouda , P. Gilot , A. Brillard , B. Stanmore, *Carbon* **38** 1011 (2000).
11. C. A. P. Zenenhoven, K. P. Yrjas, M. M. Hupa, *Ind. Eng. Chem. Res.* **35** 943 (1996).

12. "FEMLAB", multi-physics modeling package, COMSOL Ltd., Burlington, MA USA.

13. "Cell-Design", computer aided design software for modeling electrochemical cells, L-Chem, Inc., Shaker-Heights, OH USA.

NOTATIONS

A_{active}	available surface area of electrode (cm^2)
$A_{geometric}$	geometric surface area of electrode (cm^2)
C_b	concentration of dissolved oxygen in bulk solution (mol/l)
D_{O2}	bulk diffusivity of oxygen (cm^2/s)
D_{eff}	effective diffusivity of oxygen (cm^2/s)
E_{corr}	corrosion potential (V$_{NHE}$)
E_{rp}	repassivation potential (V$_{NHE}$)
E_0	reversible oxygen reduction potential (V$_{NHE}$)
F	Faraday's constant (10^5 C/g.eq.)
G_a	crevice gap height (μm)
G_f	electrolyte film thickness (μm)
i	current density (A/cm^2)
i_c	cathodic current density (A/cm^2)
i_{corr}	corrosion current density (A/cm^2)
i_o	exchange current density for O$_2$ reduction (A/cm^2)
i_L	limiting current (A/cm^2)
I_{total}	total current sustained by the cathode (A)
I_{2-D}	total current in homogeneous electrolyte without particles (A)
$I_{2-D,Area}$	total current in homogeneous electrolyte with area corrections (A)
$I_{2-D,Bruggeman}$	total current in homogeneous electrolyte with conductivity correction (A)
$I_{2-D, Area+Bruggeman}$	total current in homogeneous electrolyte with area and conductivity corrections (A)
$I_{3-D, particle}$	total current by 3-D simulation in presence of particles (A)
L_C	length of cathode (cm)
n	number of electrons transferred in reaction (g. eq./mol)
R	molar gas constant (8.314 J mol^{-1} K^{-1})
T	temperature (K)
V	potential of the electrode (V$_{NHE}$)
$V_{particles}$	volume occupied by particles only (cm^3)
$V_{solution}$	volume occupied by electrolyte only (cm^3)
$V_{geometric}$	total volume of electrolyte and particles (cm^3)

Greek Symbols

α_C	cathodic charge transfer coefficient
β	Tafel slope (mV/dec)
δ	mass transfer boundary layer thickness (cm)
$\phi_{particles}$	volume fraction of particulate
Φ	ohmic potential drop in solution (V$_{NHE}$)
κ	bulk conductivity of the electrolyte (S/cm)

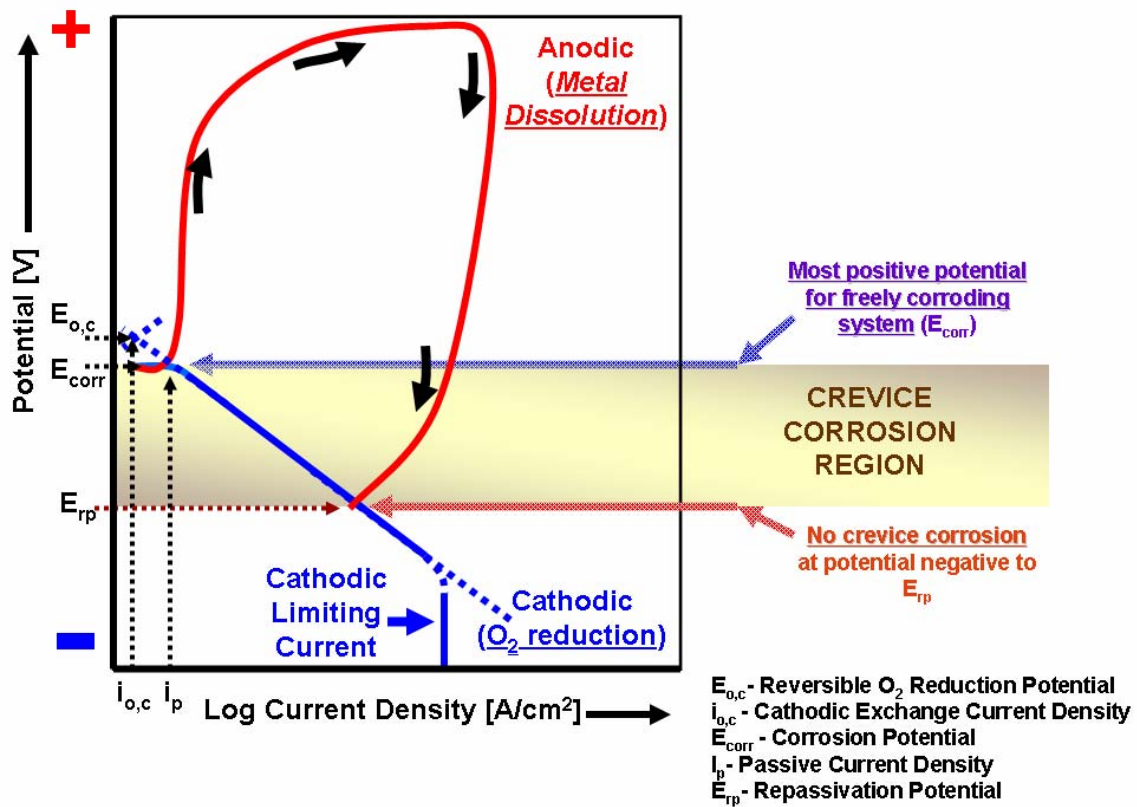| κ_{eff} | effective conductivity of the electrolyte applying Bruggeman's equation (S/cm) |
| τ | tortuosity |

FIGURES

FIGURE 1: Schematic diagram of the Cyclic Potentiodynamic Polarization curve for Stainless Steel (SS 316L) in natural seawater [5].
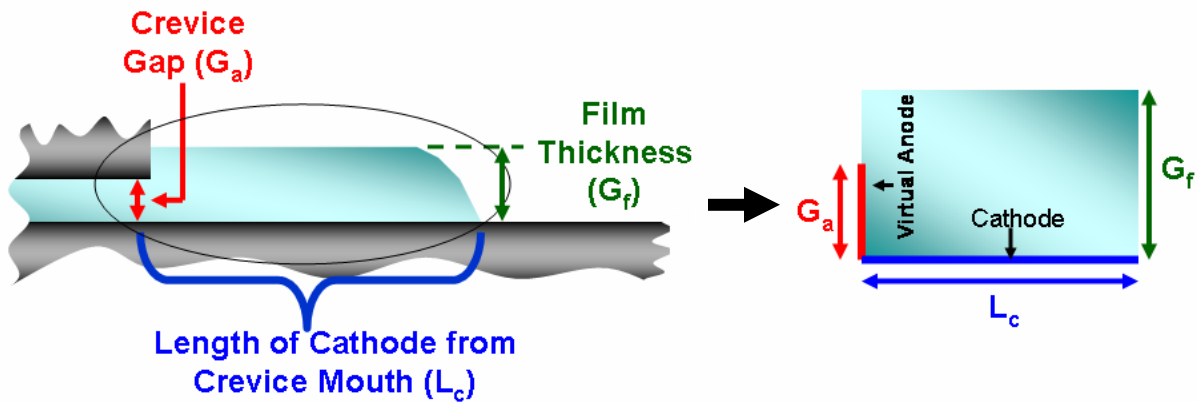

FIGURE 2: Schematic diagram of (a) a Crevice and (b) a decoupled two dimensional cathode model derived from the crevice.
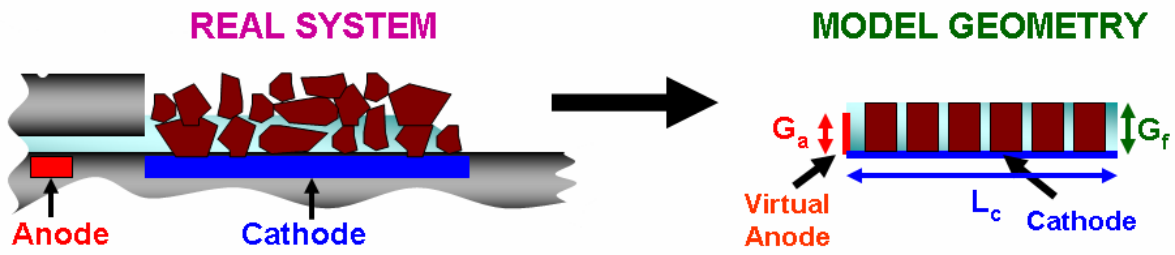
FIGURE 3: Schematic diagram of (a) crevice with the cathode covered by a thin film electrolyte with embedded particulates and (b) a decoupled cathode model with uniform particle distribution employed in simulation.
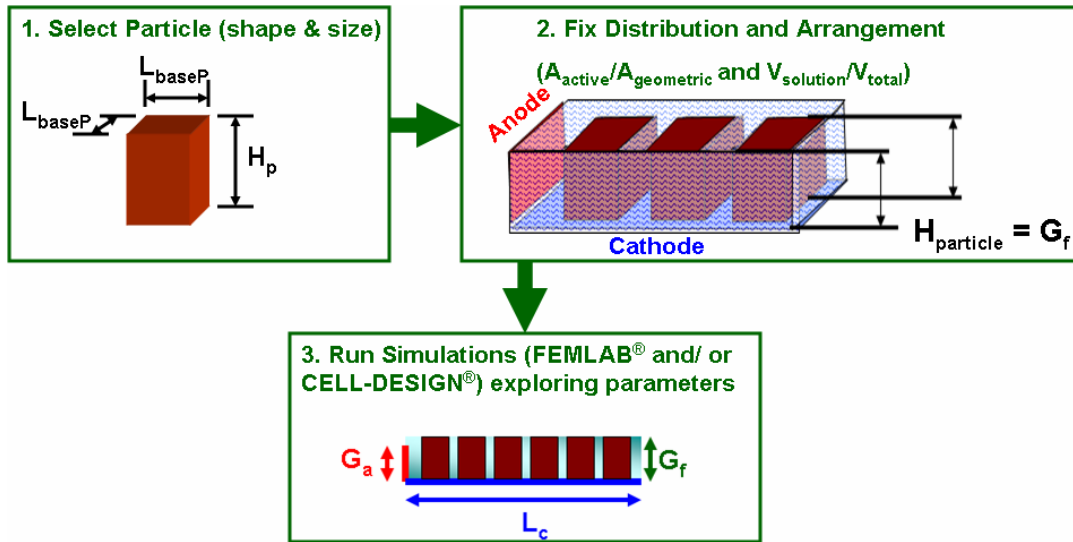
FIGURE 4: Schematic diagram of the steps involved in carrying out the simulations of particulate configurations.
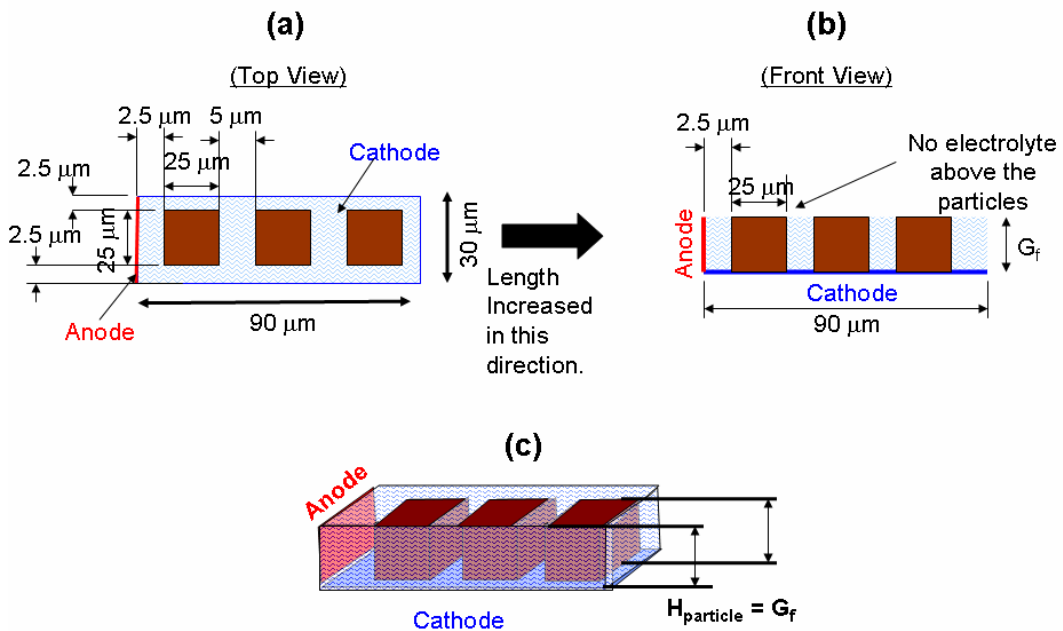
FIGURE 5: Schematic representation of uniform distribution of 25 μm cube-shaped particles on the cathode.
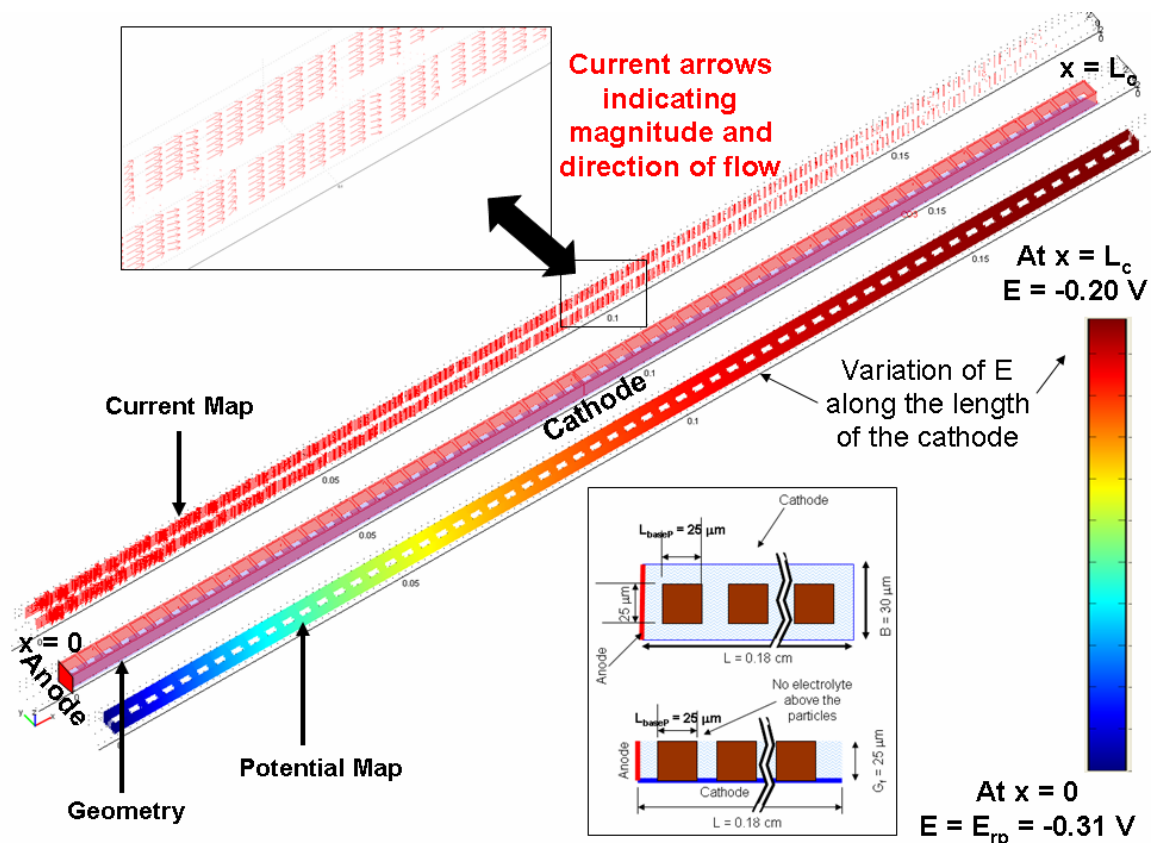
FIGURE 6: Current and potential distribution along the cathode length with a uniform distribution of 25 μm cube shaped particles. Simulation parameters are listed in Table I.
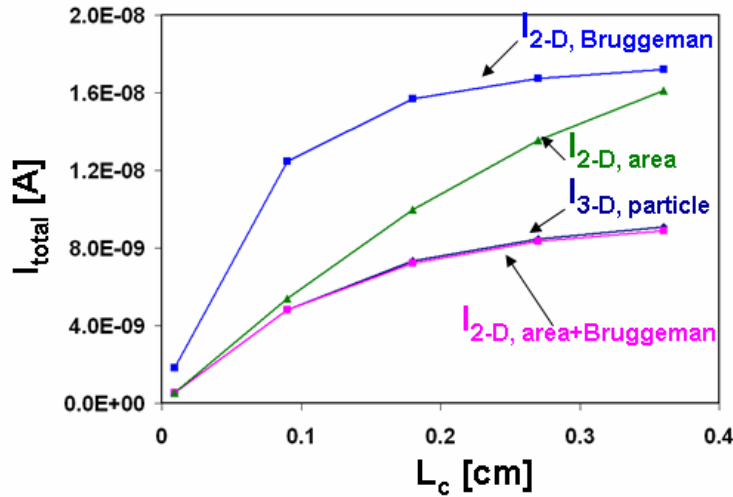
FIGURE 7: Effect of the cathode length on (i) 3-D simulated cathode capacities ($I_{3-D, particle}$) for a particulate system with the parameters of Fig.6, with the exception that $\kappa = 12.1$ mS/cm, (ii) simulated cathode capacities for homogenous electrolyte corrected only for the solution conductivity ($I_{2-D, Bruggeman}$), (iii) simulated cathode 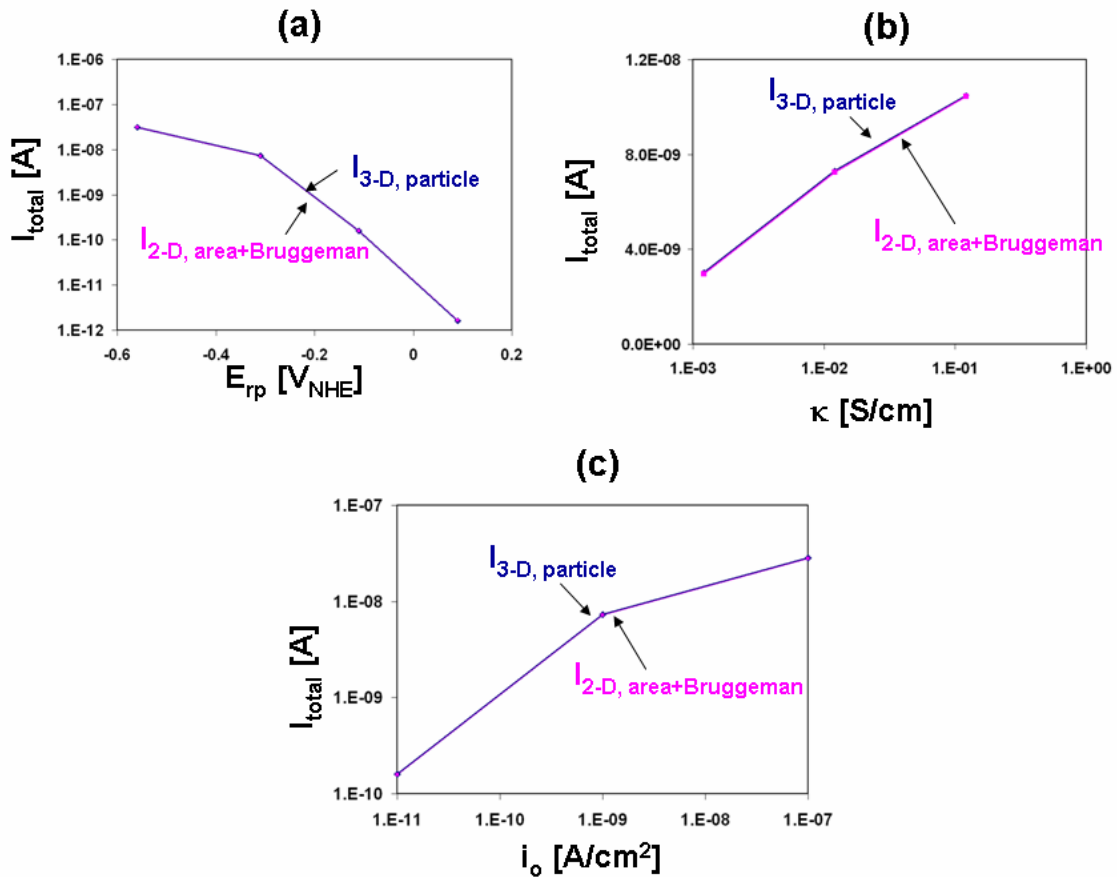capacities for homogenous electrolyte corrected only for the area coverage effect ($I_{2-D, area}$), (iv) simulated cathode capacities for homogenous electrolyte corrected for the solution conductivity and area coverage effects ($I_{2-D, area+Bruggeman}$).

FIGURE 8: Comparison of 3-D simulated cathode capacities ($I_{3-D, particle}$) for a particulate system with simulated cathode capacities for an equivalent homogenous electrolyte corrected for the solution conductivity and area coverage effects ($I_{2-D, area+Bruggeman}$) as a function of (a) variation of the repassivation potential (E_{rp}) (b) variation of the solution conductivity (κ); (c) variation of the exchange current density for oxygen reduction (i_o). Simulation parameters are identical to those of Fig. 7.
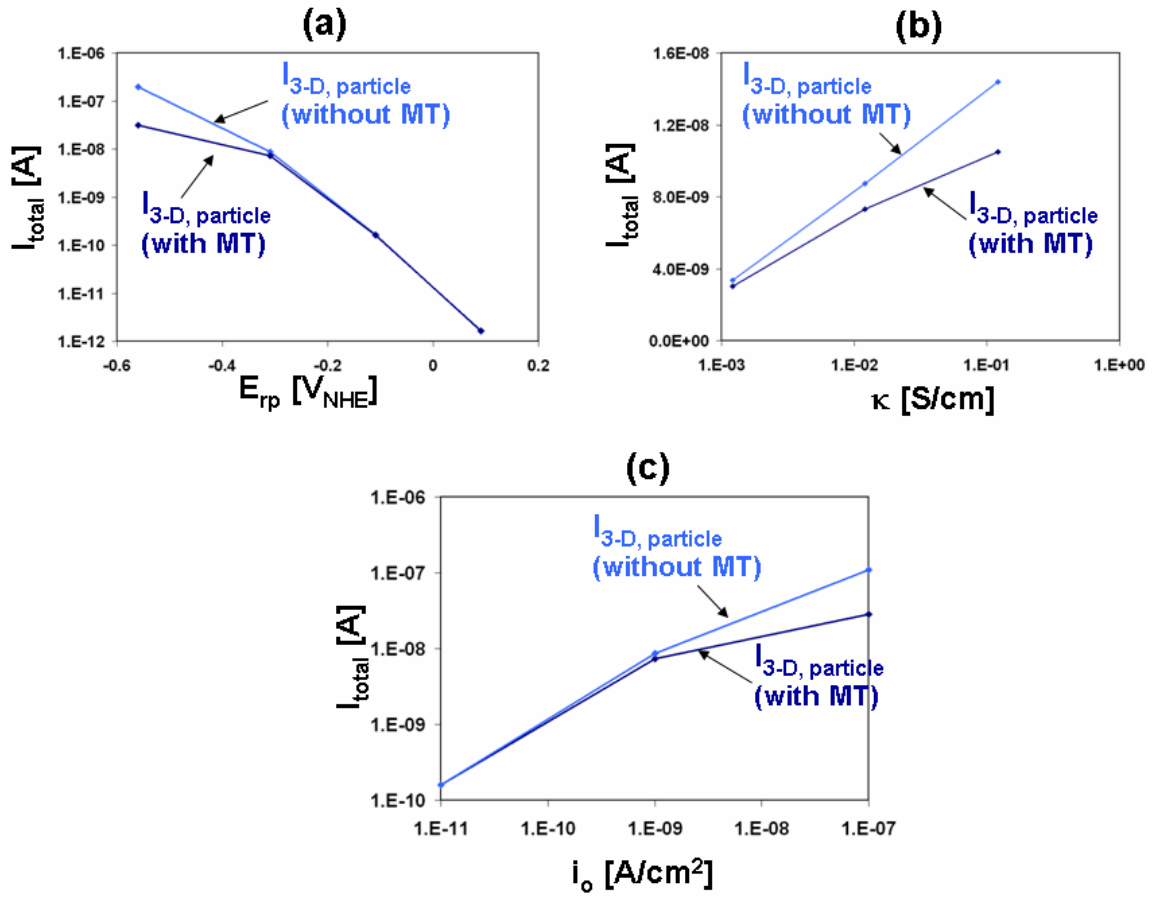
FIGURE 9: Effect of mass transfer limitation on the cathode capacity by (a) variation of the repassivation potential (E_{rp}); (b) variation of the solution conductivity (κ); (c) variation of the exchange current density for oxygen reduction (i_o). Simulation parameters are identical to those in Fig. 7.
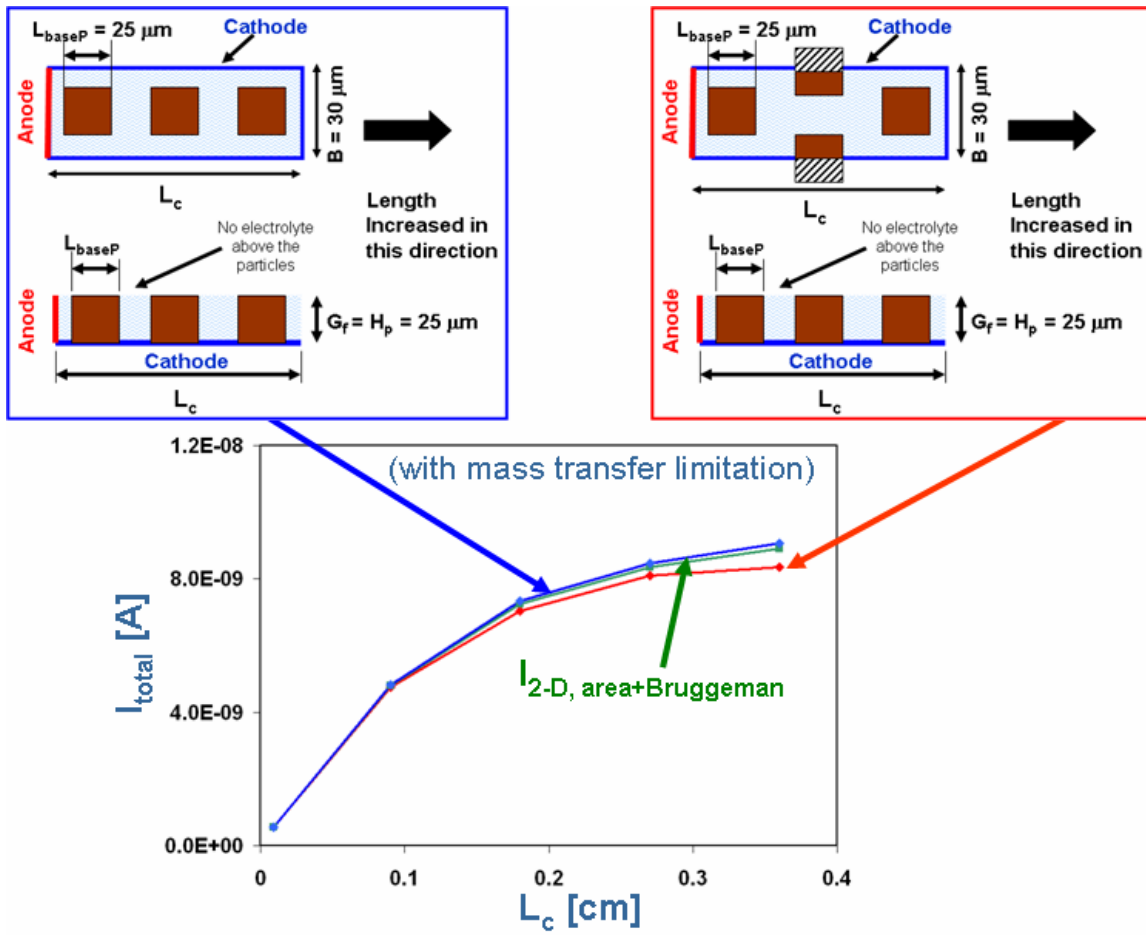
FIGURE 10: Effect of particle arrangement on the cathode capacity and comparison with 2-D simulations with particulate area and volume corrections. Modeling parameters are identical to those applied in Fig.7 and listed in Table I with the exception that $\kappa = 12.1$ mS/cm.
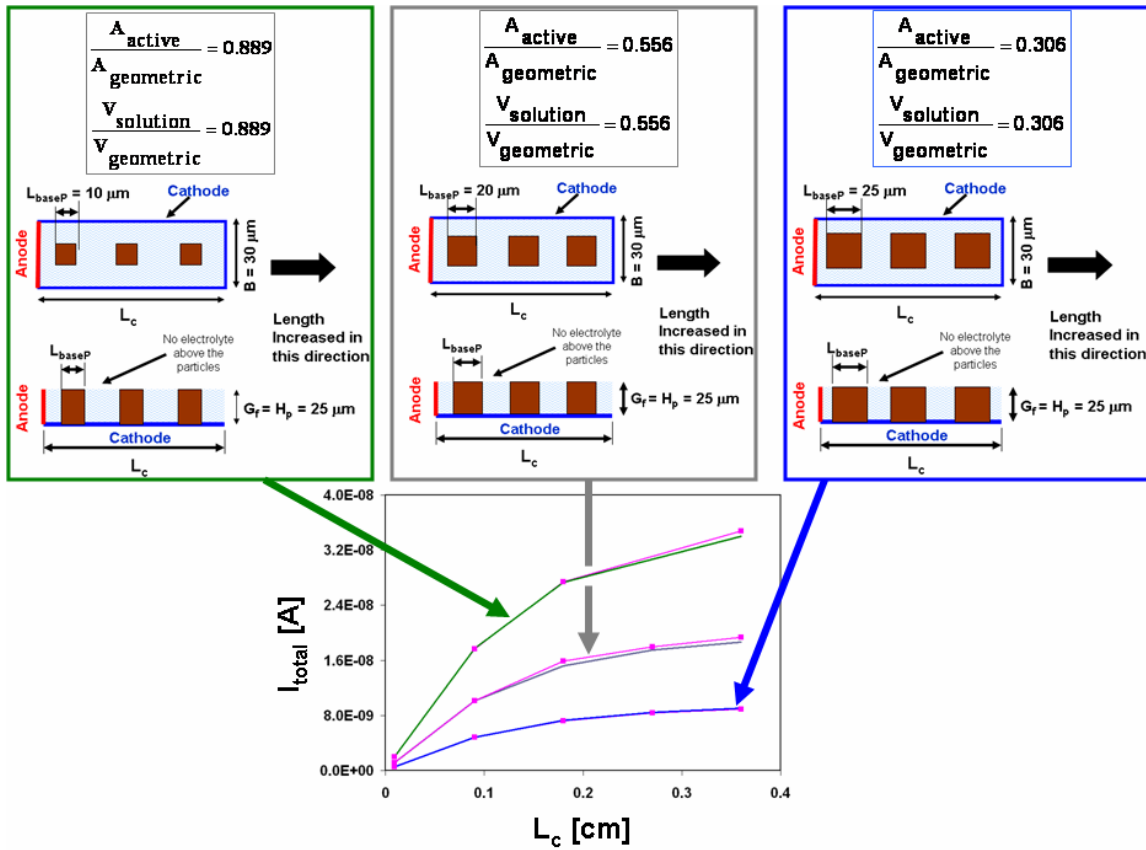
FIGURE 11: Effect of varying particulate area and volume coverage on the cathode capacity and comparison with 2-D simulations with particulate area and volume corrections. The curves in pink (-■-) indicate the simulation results obtained for an equivalent homogeneous electrolyte system with the volume and area corrections. Model parameters are listed in Table I (with the exception that κ = 12.1 mS/cm) and Table II.
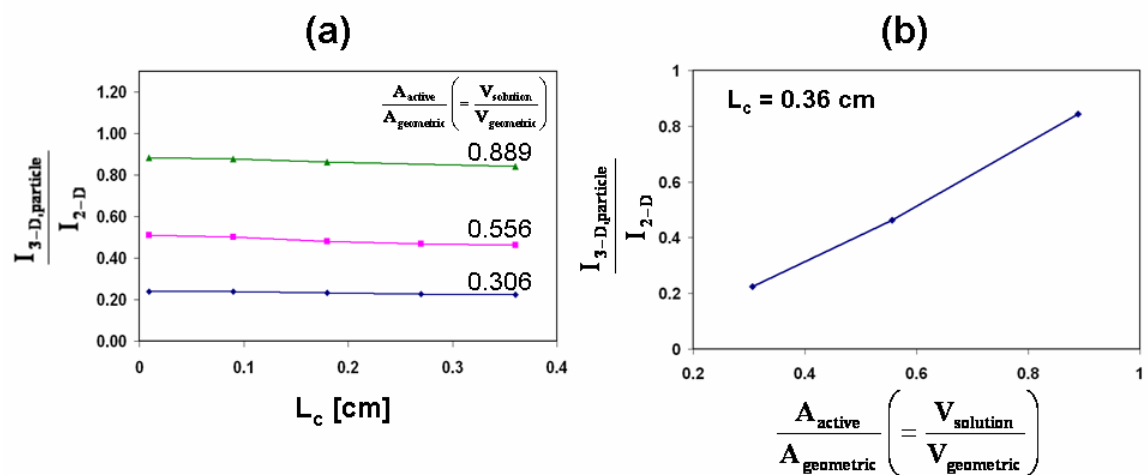
FIGURE 12: Ratio of the cathode capacity with particulates ($I_{3-D,particle}$) to that in homogeneous electrolyte without area and volume coverage corrections (I_{2-D}) plotted as a function of (a) cathode length for constant area and volume fraction coverage, and (b) area and volume fraction coverage by particles for constant cathode length of 0.36 cm. Modeling parameters are identical to those in Fig. 11.